Modeling Long-term Creep Performance for Welded Nickel-base Superalloy Structures for Power Generation Systems

Topical Report: Constitutive Creep Model for Alloy 282

DOE/NETL Cooperative Agreement
DE-FE0024027

Chen Shen
Principal Investigator
518-387-4247 (Telephone)
518-387-6232 (Fax)
E-mail: chens@ge.com

Submitted to
United States Department of Energy
National Energy Technology Laboratory
Pittsburgh, PA 15236

January 2015

GE Global Research
Niskayuna, NY 12309-1027

ACKNOWLEDGMENT

This report is based upon work supported by the Department of Energy under Award Numbers DE-FE0005859 and DE-FE0024027.

DISCLAIMER

Abstract

We report here a constitutive model for predicting long-term creep strain evolution in γ' strengthened Ni-base superalloys. Dislocation climb-bypassing γ', typical in intermediate γ' volume fraction (~20%) alloys, is considered as the primary deformation mechanism. Dislocation shearing γ' to anti-phase boundary (APB) faults and diffusional creep are also considered for high-stress and high-temperature low-stress conditions, respectively. Additional damage mechanism is taken into account for rapid increase in tertiary creep strain. The model has been applied to Alloy 282, and calibrated in a temperature range of 1375-1450˚F, and stress range of 15-45ksi. The model parameters and a MATLAB code are provided. This report is prepared by Monica Soare and Chen Shen at GE Global Research. Technical discussions with Dr. Vito Cedro are greatly appreciated. This work was supported by DOE program DE-FE0005859.

Table of Contents

Executive Summary

The heterogeneous nature in welded superalloy structures adds significant complexities to predicting creep behaviors. This is to be added to the already challenging task for predicting creep of the alloy itself over a long service life, as material's internal microstructures and deformation micro-mechanism can shift with time and alters creep strain evolution. The present program of modeling welded structures of Alloy 282 combustor liner in industrial gas turbine machine will be built upon a constitutive creep model for Alloy 282, developed previously in the DOE program DE-FE0005859 for Advanced Ultra-Supercritical (A-USC) steam turbine rotor applications. Here, this model will serve as a starting point, a 'homogeneous' part, of a more sophisticated model for welded material, where the effects of spatial gradients of chemical composition and structures and their respective time evolutions will be taken into consideration.

Given the close connection to the current program, we present here, as a Topical Report, the prior Alloy 282 constitutive creep model, together with the actual computer program and supplemental data. Aside from making this as a part of documentation for the current program, the presented technical results may also find applications in other on-going material development for advanced power generation systems.

In what follows, Section 1 summarizes the physical formulation and model parameters of the Alloy 282 constitutive creep model. It is an excerpt from the Final Report[1] of DE-FE0005859. The computer code is presented in Section 2.

Results and Discussion

1. Model Equations and Parameters

In order to capture both diffusion and dislocation mechanisms in a unified creep model we consider the total creep strain, ε^{creep}, as a superposition of dislocation component, ε^{disloc}, and diffusion component, $\varepsilon^{diffusion}$:

$$\varepsilon^{creep} = \varepsilon^{disloc} + \varepsilon^{diffusion} \tag{1}$$

1.1. Dislocation Component

For dislocation gliding and climb-bypassing precipitates, Dyson et al[2-4] proposed a hyperbolic sine dependence of the strain rate, $\dot{\varepsilon}^{disloc}$, on the net stress required to advance a dislocation:

$$\dot{\varepsilon}^{disloc} = \begin{cases} \rho A\, f(1-f)\left(\sqrt{\frac{\pi}{4f}} - 1\right) \sinh\left(C\,\frac{\sigma_{eff}-\sigma_B-\sigma_o}{MkT} b^2 \lambda\right), & \text{if } \sigma_{eff} - \sigma_B - \sigma_o > 0 \\ 0 & \text{othewise} \end{cases} \tag{2}$$

Where A and C are constant parameters, ρ is the density of dislocations, f is the volume fraction of precipitates, M is Taylor factor, k is Boltzmann constant, T is the absolute temperature, b is the Burgers vector, and λ is the average spacing between precipitates. Since each gliding dislocation encounters a series of obstacles, the net stress that drives the dislocation motion is taken as the local effective stress, σ_{eff}, subtracted by a penalty due to the interaction with other dislocations (forest dislocation strengthening term), σ_o, and a penalty due to the interaction with precipitates (back stress), σ_B. The effective stress, σ_{eff}, is further discussed in Section 1.3.

Using the Taylor law, the dislocation strengthening term is proportional to the square root of dislocation density ρ [5]:

$$\sigma_o = 0.25MG(T)b\sqrt{\rho} \tag{3}$$

where $G = E(T)/2(1+\nu)$ is the shear modulus, and ν the Poisson's ratio.

We consider that dislocation creep proceeds via either climb-bypass or shearing precipitates. For shearing precipitates with weakly coupled dislocation pairs, the back stress can be calculated as [6]:

$$\sigma_{shear} = \frac{\gamma_{APB}}{2b}\left[\left(\frac{12\gamma_{APB}fr}{\pi Gb^2}\right)^{1/2} - f\right] \tag{4}$$

Where γ_{APB} is the anti-phase boundary energy, r is the average size of precipitates. The hypothesis of the weakly coupled dislocations is made on the consideration that the space between the precipitates is large compared with their radius (about three times larger in Alloy 282). For strongly coupled dislocations σ_{shear} is expected to be slightly higher [6]. The back stress for dislocation climb-bypass, on the other hand, is calculated as[3]:

$$\sigma_{climb} = \frac{2f}{1+2f}\sigma_{eff}\left[1 - \exp\left(-\frac{1+2f}{2(1-f)}E\frac{\varepsilon^{disloc}}{\sigma_{eff}}\right)\right] \tag{5}$$

Where σ_{eff} is the effective stress, as described earlier and E is the elastic modulus.

TEM observations on the tested creep specimens indicate that the climb-bypass mechanism occurs at intermediate stress levels (20-40Ksi), and that the shear mechanism is active at higher stresses (> 40Ksi) or at high strains. For simplicity, we consider the creep deformation is driven predominantly by the weaker mechanism, either shearing or climb-bypass at a given time, although there could be a transitional regime where both are active. The back stress is thus taken as:

$$\sigma_B = \min(\sigma_{shear}, \sigma_{climb}) \quad (6)$$

A few historical TEM measurements provide an estimate of dislocation density in Alloy 282: $2 \times 10^{13}/m^2$ at 0.2% creep strain under 27.5Ksi stress, $4 \times 10^{13}/m^2$ at 0.2% strain and 32.5Ksi, and $1.4 \times 10^{14}/m^2$ at 4% strain and 32.5Ksi. Figure 1 shows TEM images of dislocation structures in Alloy 282 creep samples at 0.2% and 4% strain. We consider that the dislocation density has a linear dependence on creep strain before a constant saturation value is reached at a certain critical strain, ε^{crit}. A linear dependence of ε^{crit} on stress is fit to the above TEM data.

$$\rho = \begin{cases} \rho_f \varepsilon/\varepsilon^{crit} & \text{if } \varepsilon \le \varepsilon^{crit}(\sigma_{applied}, T) \\ \rho_f & \text{if } \varepsilon > \varepsilon^{crit}(\sigma_{applied}, T) \end{cases} \quad (7)$$

with $\varepsilon^{crit} = B\ \sigma_{applied}[MPa]$.

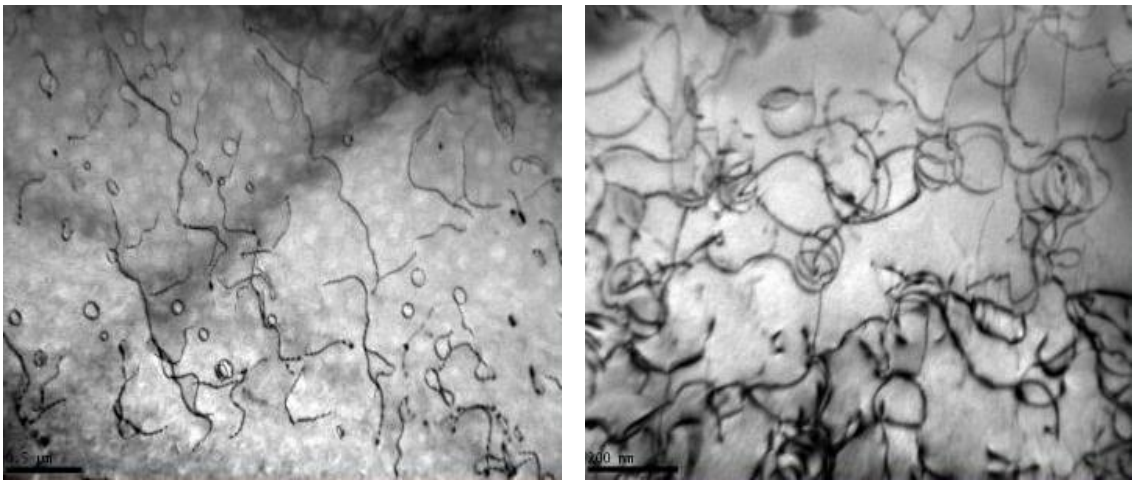

(a) (b)

Figure 1: Dislocation structures at 1400˚F at (a) 0.2% and (b) 4% creep strain. Courtesy of Mallik Karadge.

Equations (1)-(5) contain two parameters that require special attention: precipitate size and inter-space. The phase field simulations (see Final Report[1] Sections 4.1.3 and 4.1.4) showed that considerable coarsening of γ' precipitates could occur during long-term exposure to temperatures between 1300˚F and 1500˚F. Because creep also implies a long time exposure to a given temperature, an accurate evolution of the precipitate size needed to be incorporated. This was accomplished by using directly the validated phase field results for the γ' size evolution with time in the creep model. In addition, the linear relationship between the inter-particle spacing, λ, and the average precipitate size (see Final Report[1] Section 4.2) was utilized.

1.2. Diffusion component

According to Cocks and Ashby[7,8] the diffusion creep strain rate $\dot{\varepsilon}^{diffusion}$ can be contributed by multiple sources: lattice diffusion $\dot{\varepsilon}^{lattice\_diff}$, grain boundary diffusion $\dot{\varepsilon}^{boundary\_diff}$, surface diffusion at the grain boundary cavities $\dot{\varepsilon}^{cavity\_surface\_diff}$, and grain boundary diffusion near cavities $\dot{\varepsilon}^{cavity\_boundary\_diff}$:

$$\dot{\varepsilon}^{diffusion} = \dot{\varepsilon}^{lattice\_diff} + \dot{\varepsilon}^{boundary\_diff} + \dot{\varepsilon}^{cavity\_boundary\_diff} + \dot{\varepsilon}^{cavity\_surface\_diff} \quad (8)$$

The grain boundary and lattice diffusion components, which do not contribute to the cavity growth, can be written as:

$$\dot{\varepsilon}^{boundary\_diff} = 3\pi\xi\left(\frac{l}{d}\right)^3 \sigma_{applied}(1+\varepsilon^{creep}) \quad (9)$$

$$\dot{\varepsilon}^{lattice\_diff} = \xi\beta\sigma_{applied}(1+\varepsilon^{creep}) \quad (10)$$

where $\beta = \frac{3D_V}{D_B\delta_B}\frac{l^3}{d^2}$.

Considering the self-diffusivity of Ni: $D_V = 9.2\times10^{-5}\exp\left(-\frac{287kJ/mol}{RT}\right)m^2/s$ for bulk diffusion and $D_B\delta_B = 7.7\times10^{-14}\exp\left(-\frac{162kJ/mol}{RT}\right)m^3/s$ for grain boundary diffusion, reported by Divinski et. al[9], and the ratio $l/d\sim0.1$, $d = 150\mu m$, we estimated the coefficient $\beta\sim7.3\times10^{-4}$.

As discussed by Cocks and Ashby[8], the growth of cavities through diffusion is associated also with the change in the overall strain rate. The strain rate contribution due to cavities boundary diffusion is:

$$\dot{\varepsilon}^{cavity\_boundary\_diff} = \xi\frac{l}{d}\frac{\sigma_{applied}}{\ln(1/\varpi_{boundary\_diff})} \quad (11)$$

while the strain rate contribution due to cavities surface diffusion is:

$$\dot{\varepsilon}^{cavity\_surface\_diff} = \xi\alpha\frac{\sqrt{\varpi_{surface\_diff}}\sigma_{applied}{}^2}{(1-\varpi_{surface\_diff})^3} \quad (12)$$

1.3. Damage variable evolution and effective stress

Although the master equation (2) is able to describe a nonlinear increase of creep strain toward later times, tertiary creep and especially the associated grain boundary cavity growth are not well accounted for. The nucleation and growth of these voids at grain boundaries are related to a macroscopic change of the effective cross-sectional area of the creep sample, A.

Denoting by A_0 the initial cross-sectional area and by ϖ the factor related to its change: $\varpi = 1 - A/A_0$, the effective stress in the gage area of a creep specimen can be written as:

$$\sigma_{eff} = \frac{\sigma_{applied}}{(1-\varpi)}(1 + \varepsilon^{creep}) \tag{13}$$

Following [7,8,10] we assume that the cavities can grow though deformation of the neighboring grains ϖ_{disloc} or diffusion into the neighboring grains ϖ_{diff}

$$\varpi = \varpi_{diff} + \varpi_{disloc} \tag{14}$$

According to[10], the combined effects of diffusion and deformation become relevant at temperatures above half melting temperature (>1200˚F) and at stress levels beyond 10^{-3}G (i.e. 7-9Ksi at 1400 -1450˚F) for Alloy 282.

A simple linear dependence on strain is used for the dislocation component [11,12]:

$$\dot{\varpi}_{disloc} = D\dot{\varepsilon}^{disloc} \tag{15}$$

The diffusion damage variable couples the boundary diffusion component $\varpi_{boundary\_diff}$ and cavity surface diffusion component $\varpi_{surface\_diff}$:

$$\varpi_{diff} = \varpi_{boundary\_diff} + \varpi_{surface\_diff} \tag{16}$$

As proposed by Cocks and Ashby[8] the boundary diffusion damage variable evolves as:

$$\dot{\varpi}_{boundary\_diff} = \frac{\xi}{2}\frac{\sigma_{applied}(1+\varepsilon^{creep})}{\sqrt{\varpi_{boundary\_diff}}\ln(1/\varpi_{boundary\_diff})} \tag{17}$$

while the surface diffusion damage variable evolves as:

$$\dot{\varpi}_{surface\_diff} = \frac{\xi\alpha}{4}\frac{d}{\gamma}\frac{\sqrt{\varpi_{surface\_diff}}[\sigma_{applied}(1+\varepsilon^{creep})]^3}{(1-\varpi_{surface\_diff})^3} \tag{18}$$

where d is grain size, γ the surface energy, and α a scaling parameter:

$$\alpha = \frac{D_S\delta_S}{D_B\delta_B}\frac{1}{\sqrt{2}}\frac{l^2}{d\gamma} \tag{19}$$

which depends on the surface diffusion coefficient $D_S\delta_S$, boundary diffusion coefficient $D_B\delta_B$, and l, the average distance between two neighboring voids. Based on the reported diffusivities values for various materials[9] we consider $D_S\delta_S$ on the same order of magnitude as $D_B\delta_B$. Also a value of 2J/m^2 for the surface

energy and the earlier considered ratio l/d~0.1, $d = 150\mu m$ lead to an estimated value α~$0.5MPa^{-1}$.

Equations (1)-(19) constitute the proposed creep model formulation for capturing the main creep mechanisms of diffusion, dislocation climb-bypass, and to some extend particle shearing. These equations contain five parameters that have been fit to the Alloy 282 creep data at 15, 27.5, and 32.5Ksi, at 1400˚F and 1450˚F. The model parameters in Equations (1)-(19), determined by microstructural characterization, thermodynamic calculations, phase field simulations, and parameter fitting, are summarized in Table 1.

Table 1: A summary of the parameters in the creep model

Parameter name	Symbol	Value	Source
Activation volume	Ω	$1.2 \times 10^{-29} m^3$	Thermodynamic calculations
Burgers vector	b	2.54Å	Ni lattice parameter
Taylor Factor	M	3.07	Typical for FCC metal
Average grain size	d	$150\mu m$	Characterization
Void diameter/grain diameter ratio	l/d	0.1	Estimated
Lattice diffusion parameter	β	7×10^{-4}	Calculated from $\beta = \frac{3D_V}{D_B \delta_B} \frac{l^3}{d^2}$.
Self-diffusion coefficient of Ni	D_V	$9.2 \times 10^{-5} \exp\left(-\frac{287}{RT} \frac{kJ}{mol}\right)\ m^2/s$	Ref.[9]
Bulk diffusion parameter	$D_B \delta_B$	$7.7 \times 10^{-14} \exp\left(-\frac{162}{RT} \frac{kJ}{mol}\right)\ m^3/s$	Ref.[9]
Surface Energy	γ	2 J/m^2	Estimated
Anti-phase boundary energy	γ_{APB}	0.15 J/m^2	Estimated
Boundary diffusion parameter	α	$0.5MPa^{-1}$	Calculated from $\alpha = \frac{D_S \delta_S}{D_B \delta_B} \frac{1}{\sqrt{2}} \frac{l^2}{d\gamma}$
Precipitates volume fraction	f	a=(T-1033.2)/21.96 f=0.0035714a^2 - 0.011068a + 0.18774 T - temperature in K	Thermodynamic calculation
Precipitate mean radius	r	Precipitation model predictions	Precipitation model predictions
Inter-precipitates spacing	λ	λ~3r	Phase field simulation
Elastic Modulus	E	26.859T^2 - 57404T + 3.0796e+07 [MPa] T temeperature [K]	Tensile test data 1375-1450˚F
Poisson's ratio	ν	0.3	Estimated
Initial and saturation dislocation densities	ρ_f	$8 \times 10^{13}/m^2$	Microstructure observations

Creep strain rate coefficient	A	8.8E-14 1/s	Fitted
Dislocation density parameter	B	1e-5	Fitted
Creep strain rate parameter	C	0.25	Fitted
Damage evolution parameter	D	0.02	Fitted
Creep diffusion parameter	ξ	$5 \times 10^{-12} s^{-1} MPa^{-1}$	Fitted

2. MATLAB Code

The constitutive creep model for Alloy 282 is implemented in a MATLAB code. The code is applicable to uniaxial loading conditions, which correspond to that in a typical lab creep test. The code contains the calibrated parameters for Alloy 282. It has been validated against experiment for temperatures between 1375˚F and 1450˚F, and stresses between 15Ksi and 45Ksi. The output of the code is a plot of creep strain with time for a given input temperature and stress. The code can be easily modified to output other internal variable, including creep strain rate, damage parameter, and back stress.

The MATLAB code and the microstructure input files are included in the supplemental file *DE-FE0024027_TopicalReport-282CreepModel-supp.zip*, which has been provided to the Federal Project Manager.

Annotations are provided in the code below. They are started with the symbol "%". MATLAB will treat them as (non-executable) comment lines. The executable commands are written using italic, at a smaller font size.

```
% Continuum damage creep model for Alloy282 at temperature between
% 1375F and 1450F
% This Matlab code solves the continuum damage creep equations in 1D case at
% constant stress

clear all;
%
% Give the temperature in F (for Alloy282: 1375F, 1400F, 1425F or 1450F)
temper=1400;
% Give the stress in Ksi
stress_given= [15, 17.5, 20, 27.5, 32.5, 35, 37.5, 40, 45];
%
% List the fitted parameters used in the expression of dislocation strain rate
coeff_A=8.8e-14;
coeff_C=0.25;
```

```
% List fitted parameter used in the expression of dislocation density [1/um^2]
coeff_B=1e-5;
% List fitted parameter used in the expression of damage variable
coeff_D=0.02;
% List fitted parameters used in the expression of diffusion strain rate
Csi=5e-12;
%
%
% Express the Temperature in K
T=(temper - 32) * 5/9 + 273.15;
% Bolzmann constant (1.38e+23 [J/K] multiplied with temperature [K])
KT=1.38064*T;
%
% Input other material parameters or microstructural parameters
%
% Volume fraction of precipitate as a function of temperature
z = (T - 1033.2)./21.96;
f = 0.0035714.*z.^2 - 0.011068.*z + 0.18774;
%
% Elastic modulus and shear modulus [MPa] for H282 as a function of
% temperature
E_elastic=26.859.*T.^2 - 57400.*T + 3.0798e+07;
  G=E_elastic/2/(1+0.3)
%
% Burgers vector in Angstroms
bb=2.54;
Taylor_factor=3.07
% Antiphase boundary energy
APB=0.15
% Ratio between initial inter - cavities space and grain size
L_by_d=1/10;
% Grain size in microns [um]
grain_size=150
% Surface Energy in J/m^2
surf_energy=2
%
% Diffusion damage parameters
param_alpha=0.5          % [1/MPa]
param_beta=70*10^(-5)    % no units
%
Csi_alpha=Csi*param_alpha;
Csi_beta=Csi*param_beta;
%
% Initial & final dislocation density all in μm^2
rho_initial=0.0;
rho_final=80;
%
% Read the size of the stress vector and iterate through stress values
ms=length(stress_given);
```

```
%
for kstress=1:ms
%
 time =[linspace(0, 10000, 5*10^3)].*3600 ; % time in seconds
 m=length(time);
%
% Initialize a flag used for rupture criterion
 flag=0;
%
% Initialize the fields (at time=0)
% Convert the stress in MPa
stress_current= stress_given(kstress)*0.006894757*1000;
stress=zeros(m,1)+stress_current;
%
% Initialize dislocation forest hardening stress
init_stress=0.25.*E_elastic./2./(1+0.3)*bb*Taylor_factor*0.0001.*sqrt(rho_initial);
% Initialize back stress
back_stress=zeros(m,1);
%
% Read the particle size evolution with time from the precipitate model
  Particle_size=load('Prec_size1400.dat');
if temper==1375
   Particle_size=load('Prec_size1375.dat');
elseif temper==1425
  Particle_size=load('Prec_size1425.dat');
elseif temper==1450
  Particle_size=load('Prec_size1450.dat');
end
[p1,p2]=size(Particle_size);
% Initialize particle (precipitate) size
r0=Particle_size(1,2);
rad=r0+zeros(m,1);
%Initialize inter-particle distance
Lam=3.*rad;
% Initialize dislocation density
rho=zeros(m,1)+rho_initial;
%
% Initialize damage variables
omega_total=zeros(m,1);
omega_disloc=zeros(m,1);
omega_bound_diff=zeros(m,1)+1e-5;
omega_surf_diff=zeros(m,1);
%
% Initialize creep strain, strain rate
strain_disloc=zeros(m,1);
strain_diff=zeros(m,1);
strain_creep=zeros(m,1);
strainrate_creep=zeros(m,1);
%
%
% Iterate after time
```

```
for step_t=2:m
   dt=time(step_t)-time(step_t-1);
%
% Update particle size and inter-particle space
    rad(step_t) =…
interp1(Particle_size(:,1)*3600,Particle_size(:,2),time(step_t)+Particle_size(1,1)*3600);
% Extrapolate beyond the values provided in the input file
    if time(step_t)./3600>=Particle_size(p1,1)
       if temper==1375
          rad(step_t)=0.0082*(time(step_t)/3600)^ 0.3282;
          elseif temper==1425
          rad(step_t)=  0.01098*(time(step_t)/3600)^ 0.3274;
          elseif temper==1450
          rad(step_t)=  0.0161 + 0.0128*(time(step_t)/3600)^0.3250;
          elseif temper==1400
          rad(step_t)=0.0092*(time(step_t)/3600)^0.33035;
          elseif temper==1500
          rad(step_t)= 0.0160*(time(step_t)/3600)^0.3323;
          end
    end
   Lam(step_t)= 3*rad(step_t);
%
% Update dislocation strain using forward (explicit) Euler method.
% \dot{\varepsilon}^{disloc} = \rho A\, f(1-f)\left(\sqrt{\frac{\pi}{4f}}-1\right)\sinh\left(C\,\frac{\sigma_{eff}-\sigma_B-\sigma_o}{MkT}\,b^2\lambda\right),

%
    cback=2*f/(1+2*f);
   ff=f*(1-f)*(sqrt(pi/4/f)-1);
   S0=  bb*bb*Lam(step_t)*1000/Taylor_factor/KT*coeff_C ;
   xx=(1+(strain_creep(step_t-1)));

Cutting_stress(step_t)=APB/(2*bb)*10000*(sqrt(12*APB*f*rad(step_t)/10/(pi*G*bb*bb) )*10000 -
f );
% \sigma_{shear} = \frac{\gamma_{APB}}{2b}\left[\left(\frac{12\gamma_{APB}fr}{\pi Gb^2}\right)^{1/2} - f\right]
BS=min(Cutting_stress(step_t-1), back_stress(step_t-1));
%
 if (stress(step_t-1)*xx/(1-omega_total(step_t-1))-BS-init_stress)>0
     strain_disloc(step_t)=strain_disloc(step_t-1) + dt*ff*(rho(step_t-1))*coeff_A*...
    sinh(((stress(step_t-1)*xx/(1-omega_total(step_t-1))-BS-init_stress)*S0))  ;
    else
     strain_disloc(step_t)= strain_disloc(step_t-1);
 end
%
% Update diffusion strain
%\dot{\varepsilon}^{cavity\_boundary\_diff} = \xi\frac{l}{d}\frac{\sigma_{applied}(1+\varepsilon^{creep})}{\ln(1/\varpi_{boundary\_diff})},
%\dot{\varepsilon}^{cavity\_surface\_diff} = \xi\alpha\frac{\sqrt{\varpi_{surface\_diff}}[\sigma_{applied}(1+\varepsilon^{creep})]^2}{(1-\varpi_{surface\_diff})^3}
%\dot{\varepsilon}^{boundary\_diff} = 3\pi\xi\left(\frac{l}{d}\right)^3\sigma_{applied}(1+\varepsilon^{creep})
```

% $\dot{\varepsilon}^{lattice\_diff} = \xi\beta\sigma_{applied}(1+\varepsilon^{creep})$

% $\dot{\varepsilon}^{diffusion} = \dot{\varepsilon}^{lattice\_diff} + \dot{\varepsilon}^{boundary\_diff}$

% $+ \dot{\varepsilon}^{cavity\_boundary\_diff} + \dot{\varepsilon}^{cavity\_surface\_diff}$

%

```
strain_diff(step_t)=strain_diff(step_t-1)+dt*Csi*(stress(step_t-
1)*xx)*L_by_d/log(1/omega_bound_diff(step_t-1))+...
                Csi*3*pi*stress(step_t-1)*xx*(L_by_d^3) +...
                Csi_alpha*(stress(step_t-1)*xx)^2*sqrt(omega_surf_diff(step_t-1))/(1-
omega_surf_diff(step_t-1))^3+...
                Csi_beta*stress(step_t-1)*xx;
```

%

% Update total strain

```
  strain_creep(step_t)=strain_disloc(step_t)+strain_diff(step_t);
```

%

% Update back stress

% $\sigma_B = 2f/(1+2f)\sigma_{eff}(1-exp\left[-\frac{f/(1-f)E\varepsilon}{2f/(1+2f)\sigma_{eff}}\right])$

%

```
back_stress(step_t)= cback*stress(step_t)*xx/(1-omega_total(step_t))*...
  (1-exp(-f/(1-f)*E_elastic*strain_creep(step_t)/cback/(stress(step_t)*xx/(1-
omega_total(step_t)))));
```

%

% Update strain rate

```
   strainrate_creep(step_t)=(strain_creep(step_t)-strain_creep(step_t-1)) / dt;
```

%

% Update dislocation density

```
 STRAIN_DENS=stress(step_t)*coeff_B;
        if strain_creep(step_t)<=STRAIN_DENS
               m=(rho_final-rho_initial)/STRAIN_DENS;
       rho(step_t)= rho_initial + m*(strain_creep(step_t));
            else
      rho(step_t)=rho_final; %
            end
```

% Update forest hardening stress

```
init_stress= 0.25.*E_elastic./2./(1+0.3).*bb*Taylor_factor*0.0001*sqrt(rho(step_t));
```

% Update boundary diffusion damage

% $\dot{\varpi}_{boundary\_diff} = \frac{\xi}{2}\frac{\sigma_{applied}(1+\varepsilon^{creep})}{\sqrt{\varpi_{boundary\_diff}}\ln(1/\varpi_{boundary\_diff})}$

%

```
if omega_bound_diff(step_t-1)>=1
   omega_bound_diff(step_t)=1;
   else
   omega_bound_diff(step_t)= omega_bound_diff(step_t-1)+...
                                 Csi/2*dt/log(1/omega_bound_diff(step_t-…
                                 1))/sqrt(omega_bound_diff(step_t-1))*stress(step_t)*xx;
   end
```

% Update surface diffusion damage

% $\dot{\varpi}_{surface\_diff} = \frac{\xi\alpha}{4}\frac{d}{\gamma}\frac{\sqrt{\varpi_{surface\_diff}}[\sigma_{applied}(1+\varepsilon^{creep})]^3}{(1-\varpi_{surface\_diff})^3}$

%

```
 if omega_surf_diff(step_t-1)>=1
        omega_surf_diff(step_t)=1;
        else
        omega_surf_diff(step_t)= omega_surf_diff(step_t-1)+...
                        Csi_alpha/4*grain_size/surf_energy*sqrt(omega_surf_diff(step_t-1))/...
                        (1-omega_surf_diff(step_t-1))^3 * (stress(step_t)*xx)^3;
        end
% Update dislocation damage
% ω̇_disloc = D ε̇^disloc
%
 if omega_disloc(step_t-1)>=1
     omega_disloc(step_t)=1;
     else
     omega_disloc(step_t)=coeff_D*strain_disloc(step_t);
     end
% Update total damage
% ϖ = ϖ_boundary_diffdisloc + ϖ_boundary_diff + ϖ_surface_diff
%
omega_total(step_t)=omega_disloc(step_t)+ omega_bound_diff(step_t)+…
                        omega_surf_diff(step_t);
%
% Rupture criterion
%%% Ultimate stress [in Ksi] at the given temperature
 UTS=120.8;
  if omega_total(step_t)>1-stress_given(kstress)/UTS *(1+strain_creep(step_t)) & flag<1
        flag=flag+1;
        rupture_time(kstress)=time(step_t)./3600;
        rupture_strain(kstress)= strain_creep(step_t-1);
   end
%
%
end
% Plot creep strain versus time for all the given stress values
  figure(1); hold on; xlabel('Time [h]', 'fontsize',16); ylabel('Strain [in/in]', 'fontsize',16);
  xlim([0,10000]); ylim([0,0.4]);
  plot(time./3600, (strain_creep), 'r','LineWidth',2);
end
format long
% Display stress, rupture time and rupture strain at the given temperature
%%%%%   Stress [Ksi], rupture time [hours], Rupture Creep Strain
  disp  'Stress[Ksi]_______rupture_time[hours]_________Rupture_Creep_Strain'
  [stress_given', rupture_time', rupture_strain']
```

The gamma prime microstructure input for the creep model is taken as a text data file. The data file, shown below for “Prec_size1400.dat” as an example, contains two columns. The first column is the time in hours. The second column is the precipitate size in microns. All “Prec_size.dat” files need to be copied in the MATLAB working directory.

```
9.415444    0.048292
11.86831    0.0483
14.96017    0.04828
18.85753    0.048252
23.77019    0.048212
29.96278    0.048152
37.76833    0.048063
47.60778    0.047938
60.01028    0.047823
75.64361    0.0479
95.35       0.048407
120.19      0.049568
151.5014    0.051737
190.97      0.054614
240.7206    0.058404
303.4306    0.062963
382.4806    0.067168
482.1222    0.072396
607.7222    0.078769
766.0444    0.085036
965.6083    0.090857
1217.164    0.097488
1534.256    0.10684
1933.95     0.11356
2437.775    0.1232
3072.861    0.13402
3873.389    0.14351
4882.444    0.15393
6154.389    0.16543
7757.722    0.17813
9778.722    0.19214
12326.22    0.20762
15537.39    0.22474
19585.11    0.24366
24687.33    0.26456
31118.61    0.28173
39225.56    0.30686
49444.44    0.32756
62325.56    0.35782
78562.22    0.38296
99028.89    0.41027
124827.5    0.45019
157346.9    0.48371
198338.3    0.52034
250008.3    0.56045
500008.3    0.7
1000000.3   1.08
```

References

1 Shen, C. Modeling Creep-Fatigue-Environment Interactions in Steam Turbine Rotor Materials for Advanced Ultra-supercritical Coal Power Plants, A Final Report. doi:http://dx.doi.org/10.2172/1134364 (2014).

2 Dyson, B. F. Creep and Fracture of metals: mechanisms and mechanics. *Revue de Physique Appliquée* **23**, 605-613 (1988).

3 Dyson, B. F. Microstructure based creep constitutive model for precipitation strengthened alloys: theory and application. *Mat Sci. Tech* **25**, 213-220 (2009).

4 McLean, M. & Dyson, B. F. Modeling the Effects of Damage and Microstructural Evolution on the Creep Behavior of Engineering Alloys. *Journal of Engineering Materials and Technology* **122**, 273-278, doi:10.1115/1.482798 (2000).

5 Kassner, M. E. & Pérez-Prado, M. T. *Fundamentals of Creep in Metals and Alloys*. (Elsevier Science Ltd, 2004).

6 Reed, R. C. *The Superalloys, Fundamentals and Applications*. (Cambridge University Press, 2006).

7 Cocks, A. C. F. & Ashby, M. F. Intergranular fracture during power-law creep under multiaxial stresses. *Metal Science* **14**, 395-402, doi:10.1179/030634580790441187 (1980).

8 Cocks, A. C. F. & Ashby, M. F. On creep fracture by void growth. *Progress in Materials Science* **27**, 189-244, doi:http://dx.doi.org/10.1016/0079-6425(82)90001-9 (1982).

9 Divinski, S. V., Reglitz, G. & Wilde, G. Grain boundary self-diffusion in polycrystalline nickel of different purity levels. *Acta Materialia* **58**, 386-395, doi:http://dx.doi.org/10.1016/j.actamat.2009.09.015 (2010).

10 Needleman, A. & Rice, J. R. Plastic creep flow effects in the diffusive cavitation of grain boundaries. *Acta Metallurgica* **28**, 1315-1332, doi:http://dx.doi.org/10.1016/0001-6160(80)90001-2 (1980).

11 Hayhurst, D. R., Lin, J. & Hayhurst, R. J. Failure in notched tension bars due to high-temperature creep: Interaction between nucleation controlled cavity growth and continuum cavity growth. *International Journal of Solids and Structures* **45**, 2233-2250, doi:http://dx.doi.org/10.1016/j.ijsolstr.2007.11.026 (2008).

12 Perrin, I. J. & Hayhurst, D. R. A method for the transformation of creep constitutive equations. *International Journal of Pressure Vessels and Piping* **68**, 299-309, doi:http://dx.doi.org/10.1016/0308-0161(95)00069-0 (1996).